

Electronic Supporting Information

Section 1 Effect of on-site Coulomb interaction to the intercalation voltages by GGA + U approach

Table S2 and Figure S1 show reaction voltage for Li intercalation into garnet LLTaO as a function of effective on-site Coulomb potential U using GGA-PBE + U functional. The intercalation voltage increases monotonically with U , but is negative even at $U = 5.0$ eV, which is typical for late 3d transition metals (see main text).

Table S2 Intercalation voltages as a function of effective on-site Coulomb potential U for garnet LLTaO

U /eV	Intercalation voltage /V
0.0	- 1.03
3.0	-0.68
5.0	-0.25

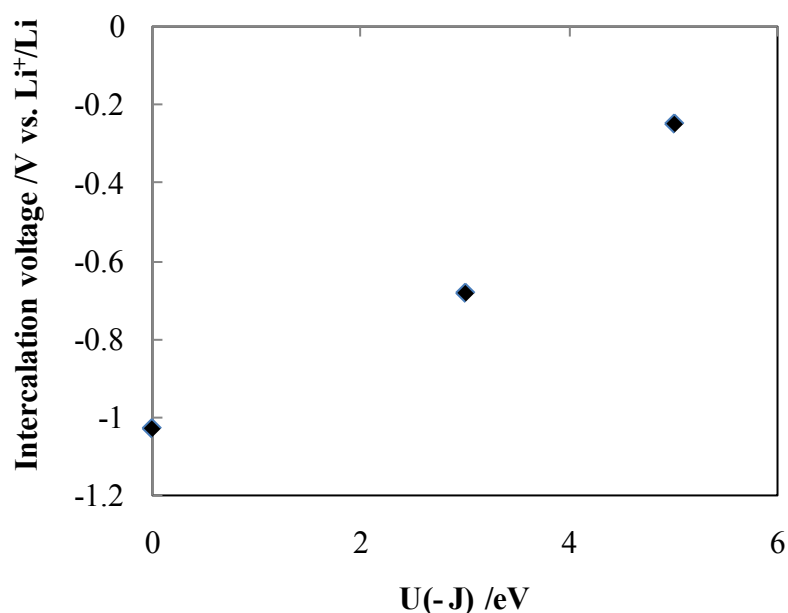


Figure S1 Intercalation voltages as a function of effective on-site Coulomb potential U for garnet LLTaO

Section 2 XRD and SEM images of garnet LLTaO and perovskite LTaO before and after a contact with molten Li

As shown in Fig. S2(a), the XRD patterns of garnet LLTaO were unchanged after contact with molten Li, which supports non reactivity of garnet LLTaO shown in Fig. 3 (a). Likewise, XRD pattern of perovsite LTaO shows no significant change after Li contact, except for minor peaks (see arrows), even after reduction reaction proceeded as shown in Fig. 3(b). Hence, the reduction of perovskite LTaO can be interpreted by intercalation mechanism. SEM images of both compounds also indicate no marked modification of morphology of sintered materials after the contact of molten Li. (Fig. S3)

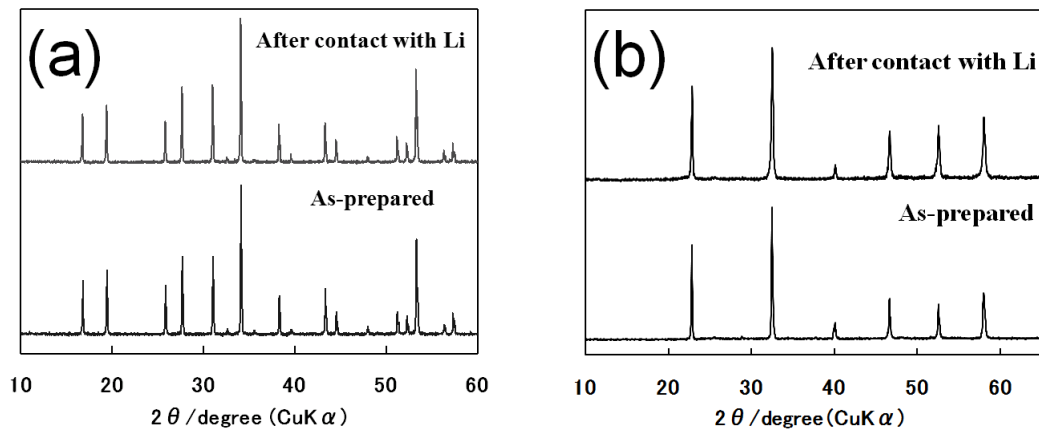


Figure S2 Changes in X-ray diffraction patterns before and after reaction for (a) garnet LLTaO ($\text{Li}_5\text{La}_3\text{Ta}_2\text{O}_{12}$) and (b) perovskite LTaO ($\text{La}_{1/3}\text{TaO}_3$) with molten Li metal.

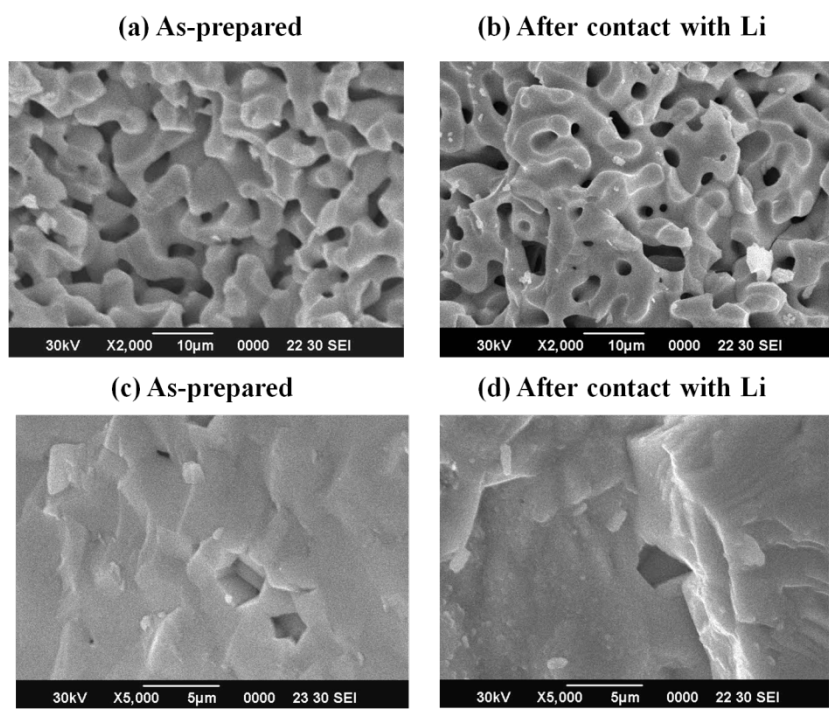


Figure S3 SEM images of (a,b) garnet LLTaO and (c,d) perovskite LTaO before and after contact with molten Li.

Section 3 XRD patterns of perovskite LTaO before and after electrochemical Lithiation

Fig. S4 show the XRD patterns for perovskite LTaO before and after electrochemical lithiation.

Corresponding voltage profiles are shown in Fig. 4 in Main text. The electrode was a mixture of 85 wt % perovskite LTaO powder, 7 wt % acetylene black, 3 wt % PTFE, and Ni powder as internal standards for XRD measurements. Electrochemically lithiated samples for XRD measurements were prepared as follows; Li ions were inserted into pristine $\text{La}_{1/3}\text{TaO}_3$ electrodes by slow galvanostatic discharging up to 0.5 V vs. Li^+/Li at a rate of 0.1 C, and then the voltage was maintained at 0.5 V for 24 hours to complete the lithiation. After the reaction, the sample was rinsed with EC-DEC solvent to remove Li salt. The lithiated samples are covered with polyethylene (PE) film to protect them from air and moisture.

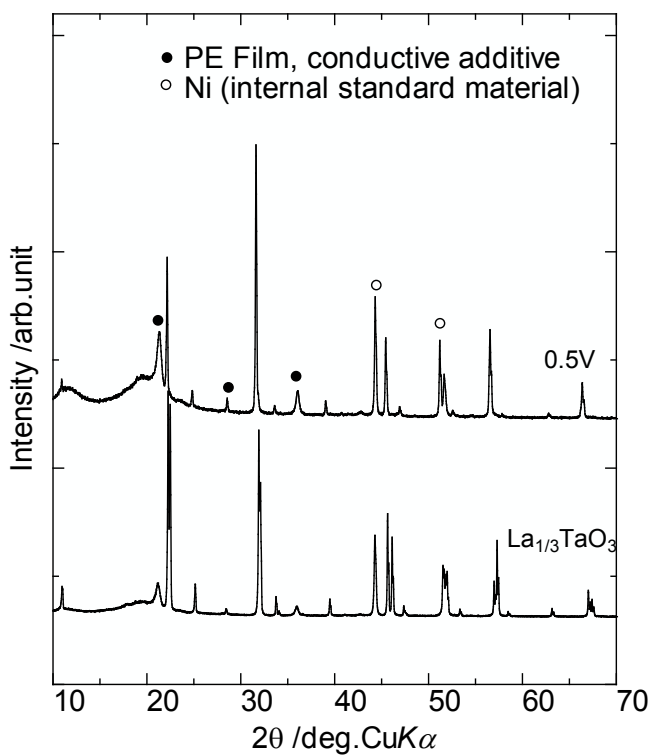


Figure S4 XRD patterns of perovskite LTaO before and after electrochemical lithiation.

Section 4 Influence of covalent character on Li ion conductivity in a Garnet-type $\text{Li}_7\text{La}_3\text{Zr}_2\text{O}_{12}$ by using molecular dynamics simulation

Classical molecular dynamics simulation (MD) was used to investigate influence of covalent character on lithium ion conductivity in a garnet-type $\text{Li}_7\text{La}_3\text{Zr}_2\text{O}_{12}$ (LLZO). The force field (FF) parameters modeled with Buckingham potential are listed in Table S3 by referring to literatures.^{1,2} To reproduce the covalent character, partially ionic model (PIM) was used, in which effective charge of Zr and O ions are modified, as reported in ref. 3. In the present study, we assume in the effective charge of Zr was set as + 3.4 (85 % against fully charged state of Zr^{4+}), and the effective charge of oxide ion was – 1.9 to compensate the charge neutrality. For the comparison purpose, fully ionic model (FIM) is also calculated, in which the effective charges of Zr and O ions are consistent with nominal ones, +4 and – 2.0, respectively. DL_POLY 4 software package⁴ was used for supercells of $3 \times 3 \times 3$ unit cell (5184 atoms) of the reported phase.⁵ Firstly, constant pressure (NPT) ensemble was applied to predict the equilibrium lattice parameters using FIM for 500 ps, and then a constant volume (NVT) ensemble to predict the diffusion properties with volume of the cell set to the equilibrium value for the given temperature for FIM and PIM. The diffusion coefficient is calculated as the averaged mean square displacement (MSD) of Li atoms over time. Convergence of diffusion coefficients is achieved with approximately 500 ps above 800 K.

Figure S5 displays Arrhenius plots of diffusion coefficients for LLZO with FIM and PIM. Present results show higher diffusivity in FIM than in PIM. In addition, activation energy of FIM (~ 0.17 eV) is lower than that of PIM (~0.21 eV). Therefore, fully ionic character in LLZO is beneficial in terms of improvement of Li ionic conductivity as well as electrochemical stability against Li metal as mentioned in main text. However, present calculation only considers the difference in effective charge of transition metal and oxide ion (Zr and O in this case). To clarify the influence of covalent character on Li ion conductivity in LLZO precisely, we are presently calculating the Li diffusion property by using ab initio molecular dynamics.

Table S3 Buckingham interionic potential parameters

Interaction	A_{ij} /eV	ρ_{ij} /Å	C_{ij} /eV Å ⁶	Reference #
Li ⁺ -O ²⁻	828.01	0.2793	0.0	1
La ³⁺ -O ²⁻	2088.79	0.3460	23.25	2
Zr ⁴⁺ -O ²⁻	1502.11	0.3477	5.10	2
O ²⁻ -O ²⁻	9547.96	0.2192	32.0	1, 2

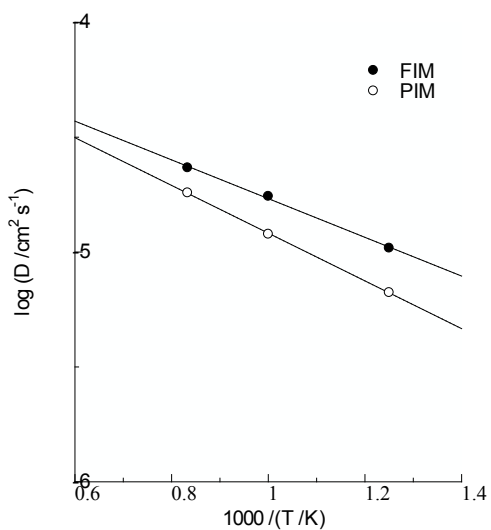


Figure S5 Arrhenius plot of diffusion coefficient of Li ion in Li₇La₃Zr₂O₁₂ obtained by classical MD simulation with FIM and PIM.

References

1. D. J. Binks, Ph. D. Thesis, Chemistry Department, University of Surry, Oct **1994**.
2. L. Minervini, R. W. Grimes, K. E. Sickafus, *J. Am. Ceram. Soc.* **2000**, *83*, 1873.
3. T. Katsumata, Y. Inaguma, M. Itoh, K. Kawamura, *Chem. Mater.* **2002**, *14*, 3930.
4. I. T. Todorov, W. Smith, K. Trachenko, M. T. Dove, *J. Mater. Chem.* **2006**, *16*, 1911.
5. C. A. Geiger, E. Alekseev, B. Lazic, M. Fisch, T. Armbruster, R. Langner, M. Fechtelkord, N. Kim, T. Pettke, W. Weppner, *Inorg. Chem.* **2011**, *50*, 1089.